# The X-arm interferometer test of HEPI at LIGO Livingston

J. Giaime, Louisiana State University & LIGO Livingston.

# Development history

- *Decades of R&D* on quiet hydraulics with Dan DeBra at Stanford, focussing on use of laminar flow oil to actuate machine tool assemblies.
- Recent development & *prototyping of zero-stiction balanced bellows quiet hydraulic actuators*, by DeBra, Hardham, Lantz et al, intended for use in Advanced LIGO pre-isolation stage. 2-DOF test stand experiment.
- Study by Hua et al of effective *control filter techniques* for 'sensor correction' active seismic isolation at sub-hertz frequencies.
- *Design of third-generation* actuator, payload suspension springs, and external housing for HEPI by Hardham, Hammond, Mason, Kern, Lacour, etc.
- *Tests at LASTI* (ongoing) by Mason, Hardham, Coyne, Lantz, Mittleman, Ottaway, Sarin, Macinnis, etc. New 'safe' fluid in use, tested at CIT.
- *Re-implementation of control system* and electronics for LIGO/VME environment and GDS by Bork, Sarin, Abbott(s), etc.
- *Mass production and installation* at LLO, by Kern, Abbott, Spjeld, Lacour, Traylor, Overmier, Mailand, Hanson, Carter, and many more.
- *Hardware/software commissioning at LLO* by Abbott, Traylor, Overmeir, Hanson, Fyffe, Wooley, Sellars, Parameswariah, etc.
- *Controls commissioning/ testing at LLO* by Mittleman, O'Reilly, Coyne, Lantz, Giaime, Frolov, etc.

# Active noise reduction

## Feedback

$$\begin{aligned} y =& (I+GK)^{-1}GK\,r \quad \text{command tracking} \\ &+ (I+GK)^{-1}G_\mathrm{d}\,d \quad \text{disturbance suppression} \\ &- (I+GK)^{-1}GK\,n. \quad \text{noise} \end{aligned}$$

## Feedforward

$K_\mathrm{ff}G_\mathrm{ff}G = G_\mathrm{d} \Rightarrow$ noise cancellation

## Sensor Correction

$M$ corrects error signal within servo loop

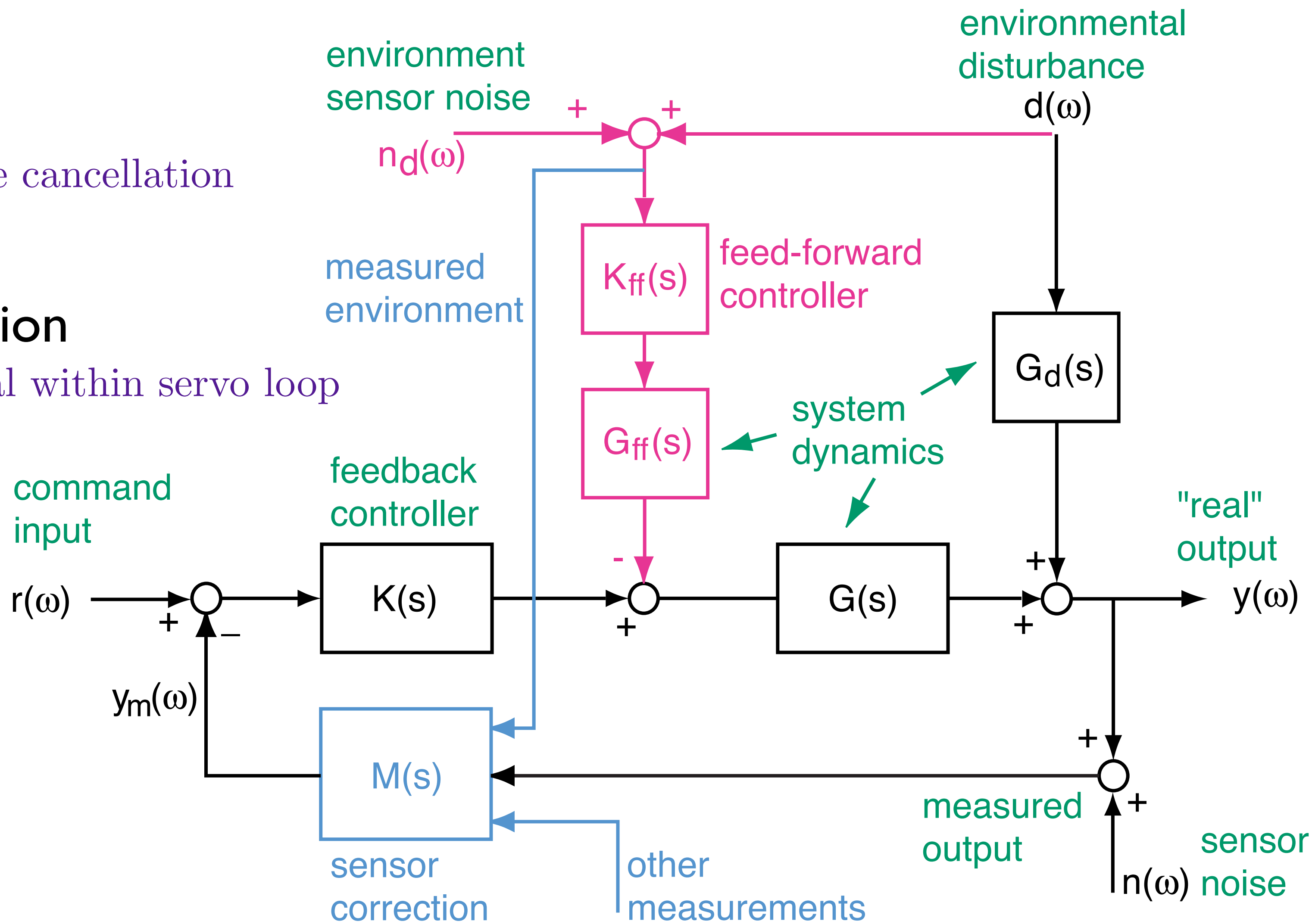

# Low-frequency pre-isolation

- At each tank corner pier, there is a sensor/actuator set, vertical and horizontal.
- Each DOF controlled with respect to HEPI displacement sensors and geophones.
- Displacement sensor corrected for floor motion as measured by Streckeisen STS-2., in x, y, z DOF's.

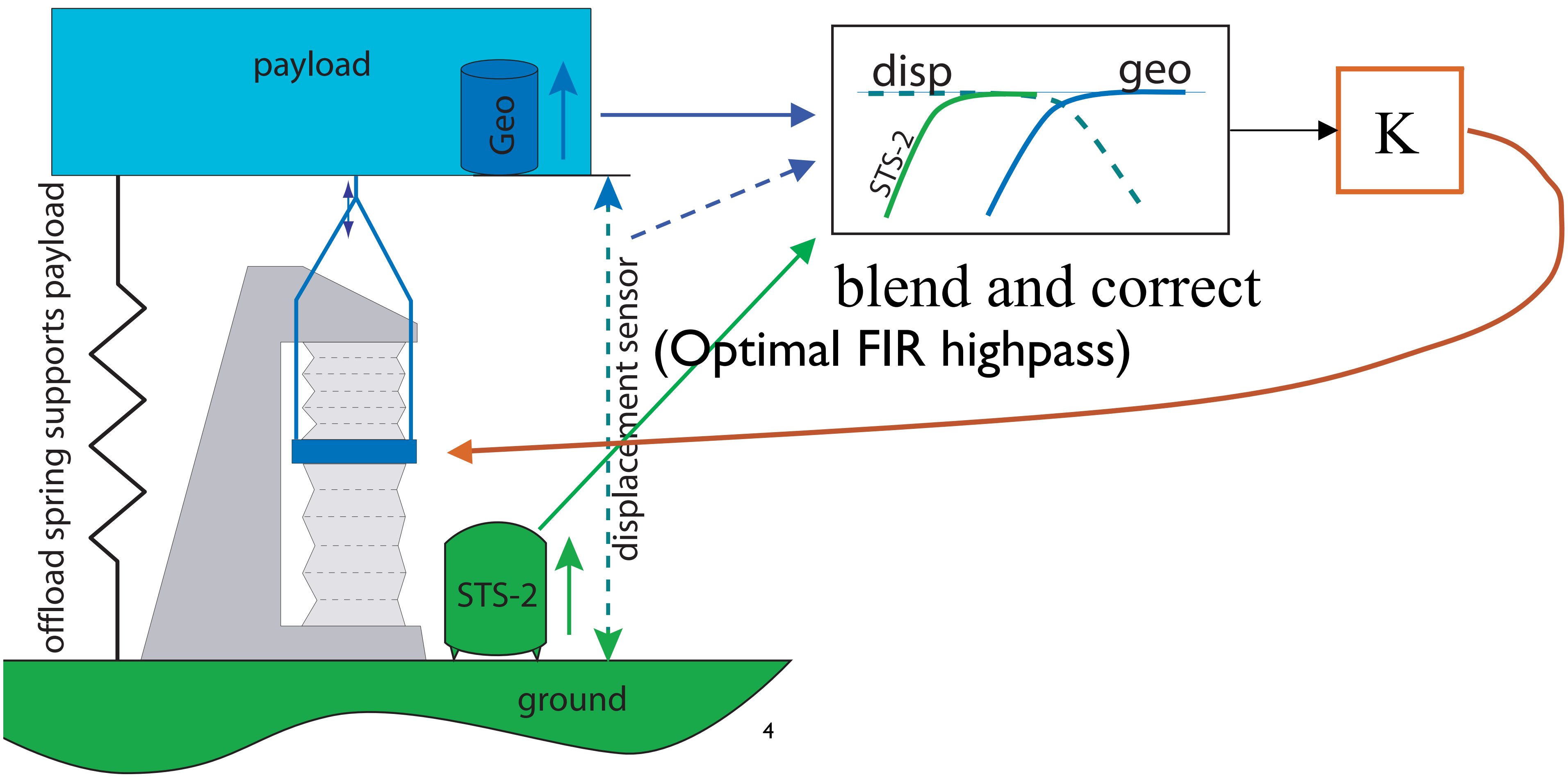

# Hydraulic bridge actuation

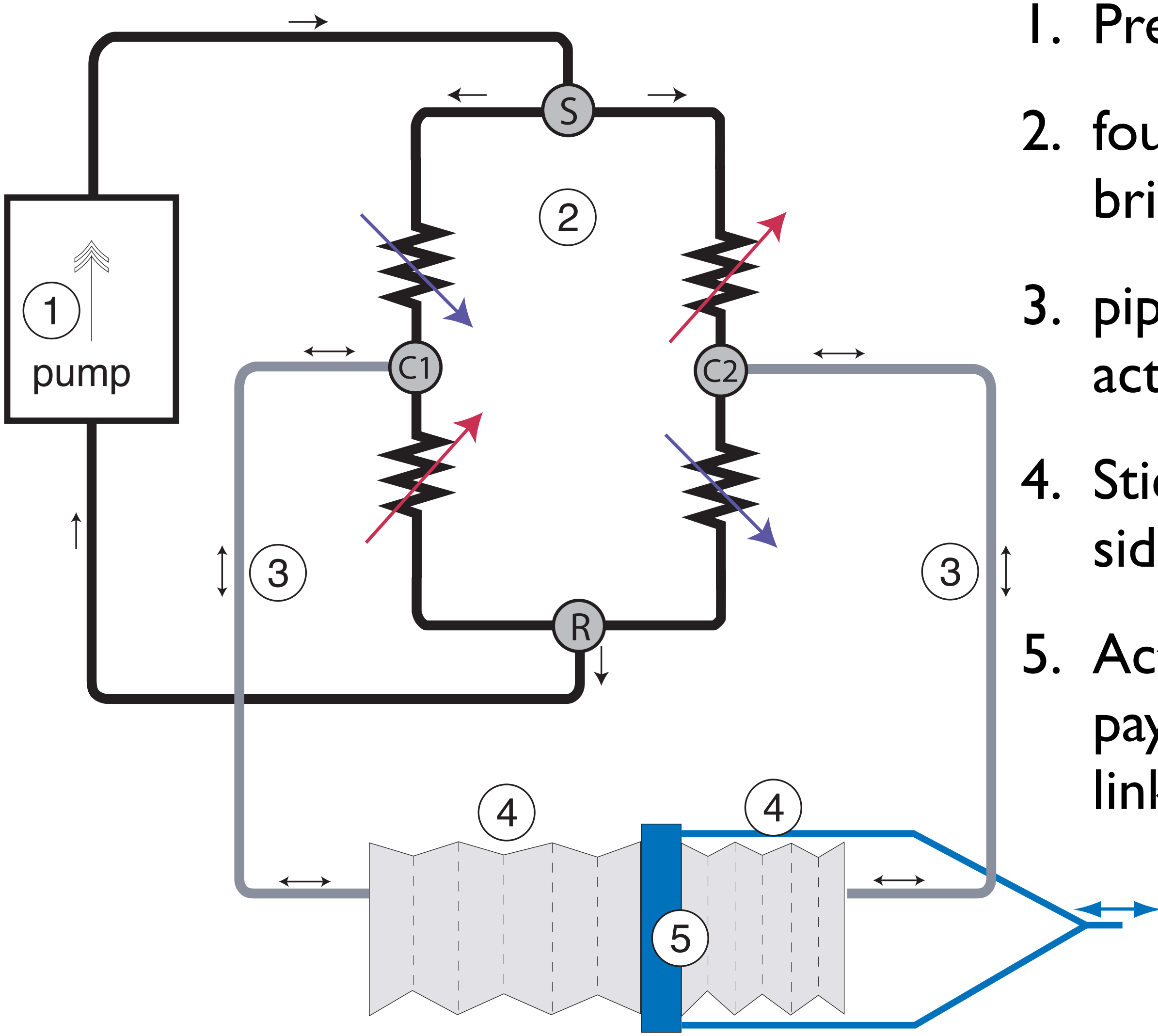


1. Pressure-stabilized pump.
2. four-valve flow-resistance bridge.
3. pipes connect bridge to actuator.
4. Stiction-free bellows on each side of actuated plate.
5. Actuated plate connected to payload through 1-DOF linkage.

# Valve issues

- Electrically-controlled valve bridge is central to the design.
- Three valve-related failure modes have been observed.
  - Gross imbalance in actuation with zero drive; may be due to particles in the fluid path or blocking the armature. In some cases this has shown to be leakage in the non-valve parts of the actuator.
  - abnormally low 'gain.' Not understood, but may be due to crud or particles.
  - oscillation (due to too-high fluid pressure.)

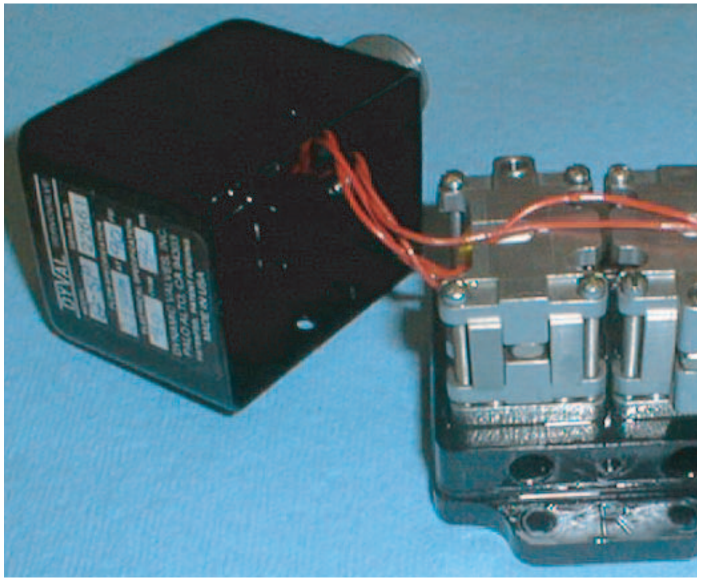

Parker DYP-2S valve

Flow in the DYP-2S

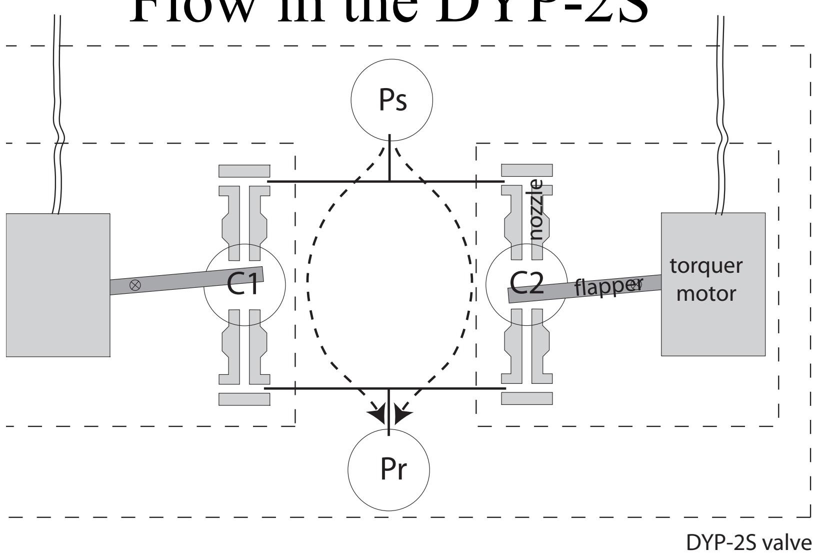


The new nozzle

# Installation and Commissioning

# Pier actuation system

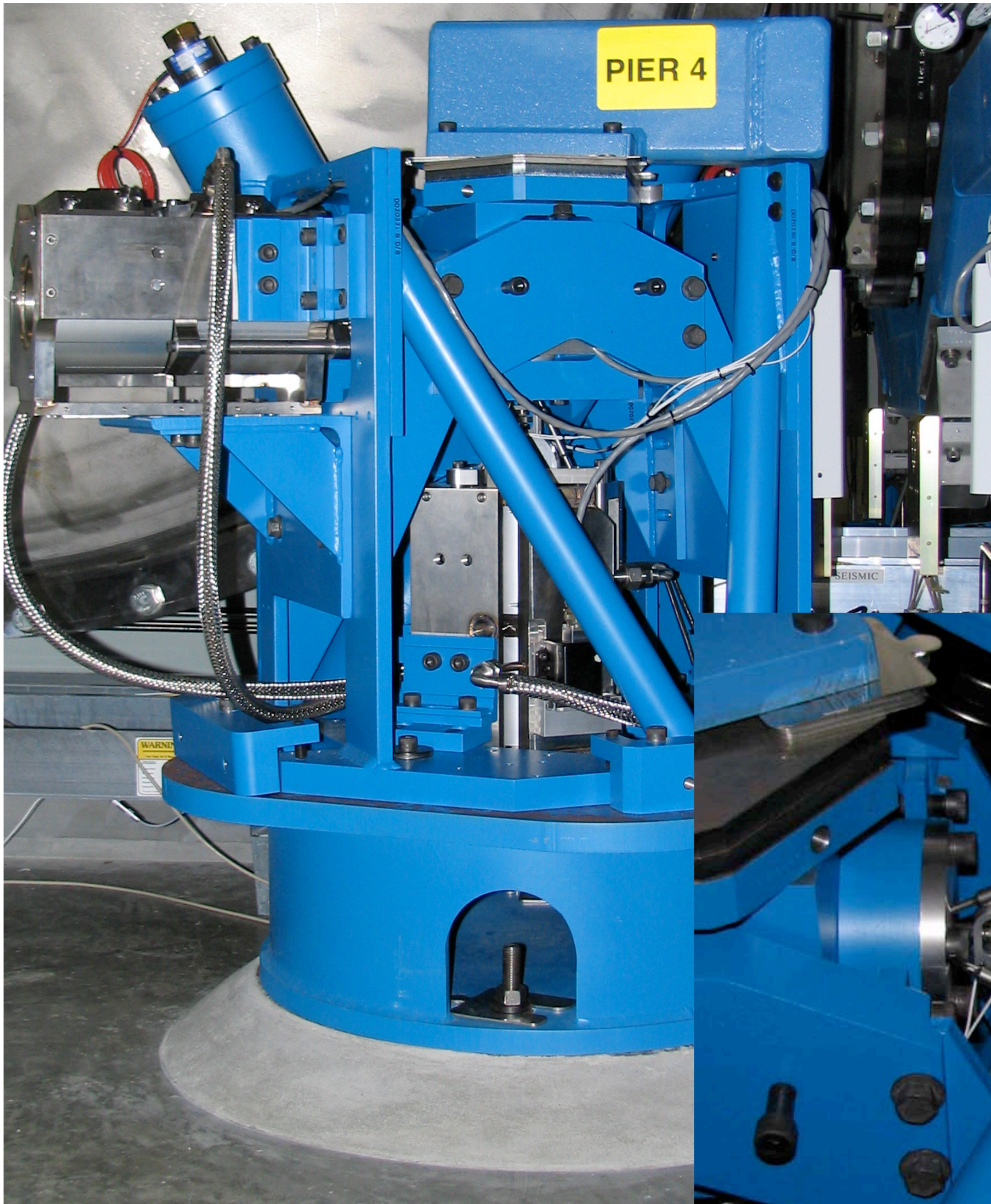


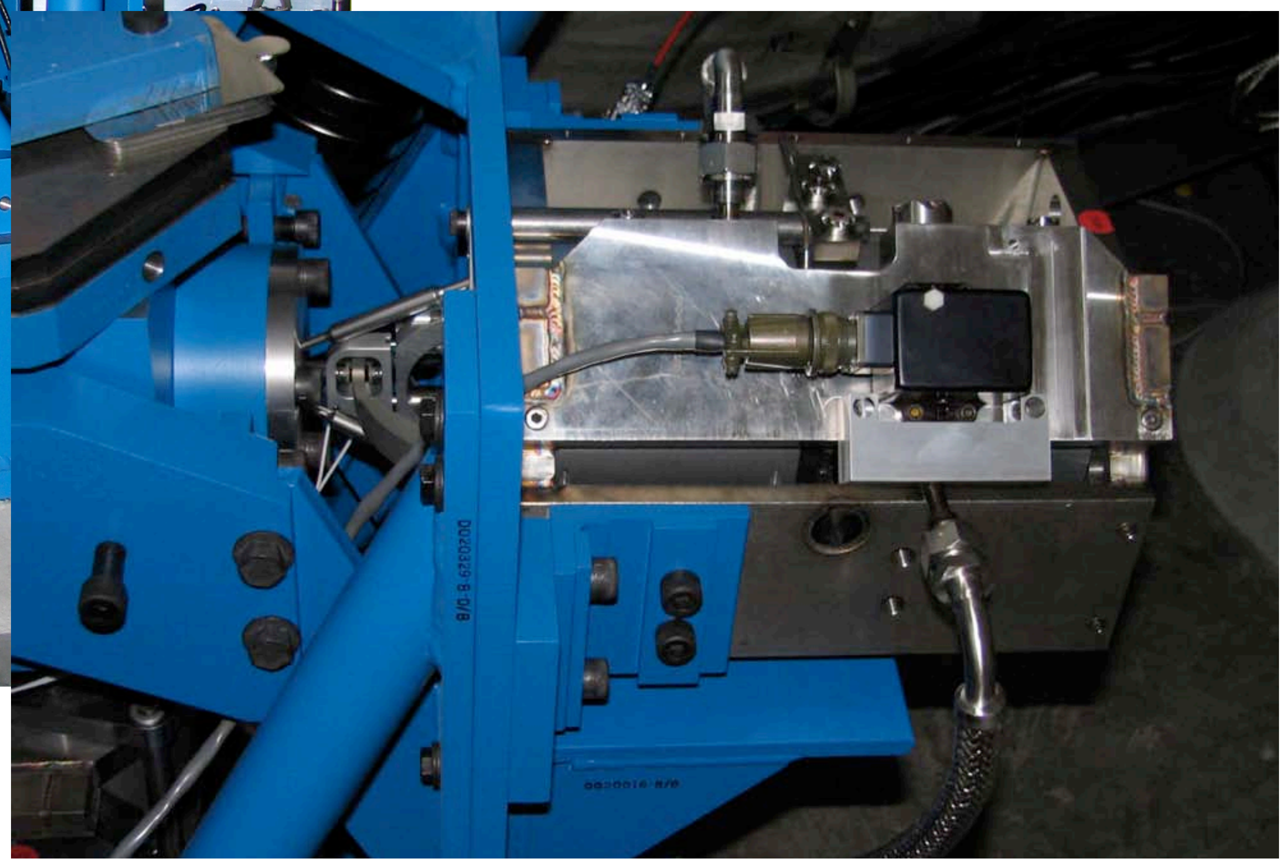

# LVEA pump stations

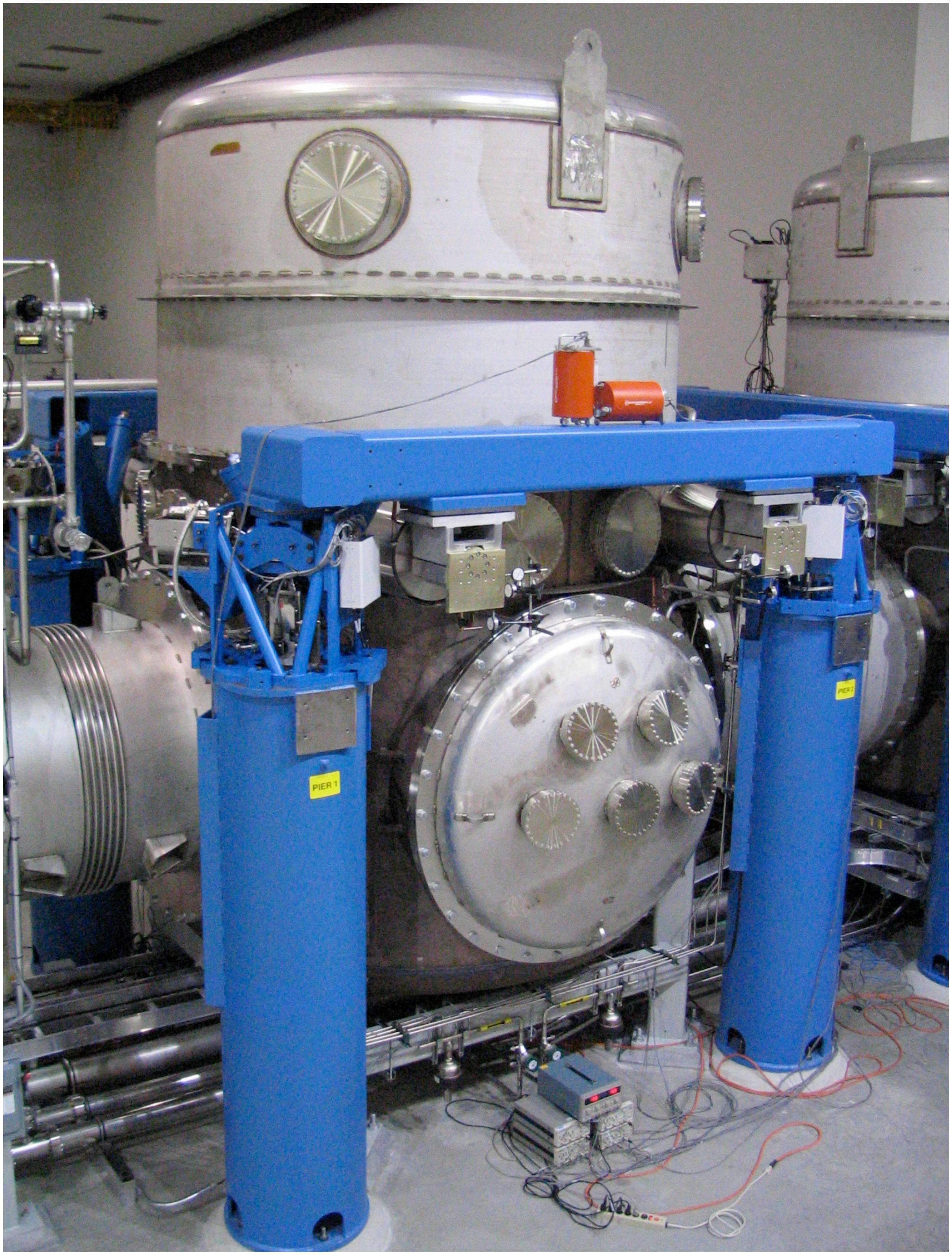


# Commissioning procedure

1. Manual sensor & actuator check-out, platform alignment.
2. Automated system identification of 8 input, 16 output, plant.
3. Feedback servo design and implementation for x, y, z, rx, ry, rz and two overconstrained DOFs.
4. Sensor correction sys-id, using portable witness geophones.
5. Sens. correction filter design and implementation for x, y, z.

# Polyphase highpass FIR for sensor correction (W. Hua)

- Seismometers cannot easily distinguish between horizontal acceleration and ground tilt & thermal artifacts.
- Below 0.1 Hz, there is very little coherence between STS-2 seismometer signals and the LIGO detector DOFs.
- Challenge: low-frequency cut-off of seismometer-based sensor correction signal, to avoid tilt and thermal pickup from seismometer. This filter should roll up as steeply as possible, while allowing magnitude and phase accuracy above 0.1 Hz
- Hua's design implemented by R. Bork for LIGO/vx-works front end code.

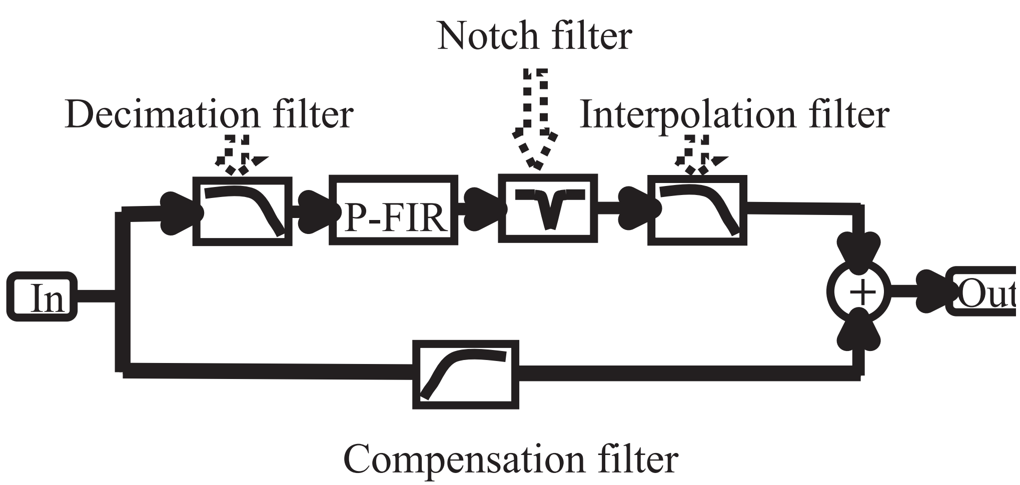


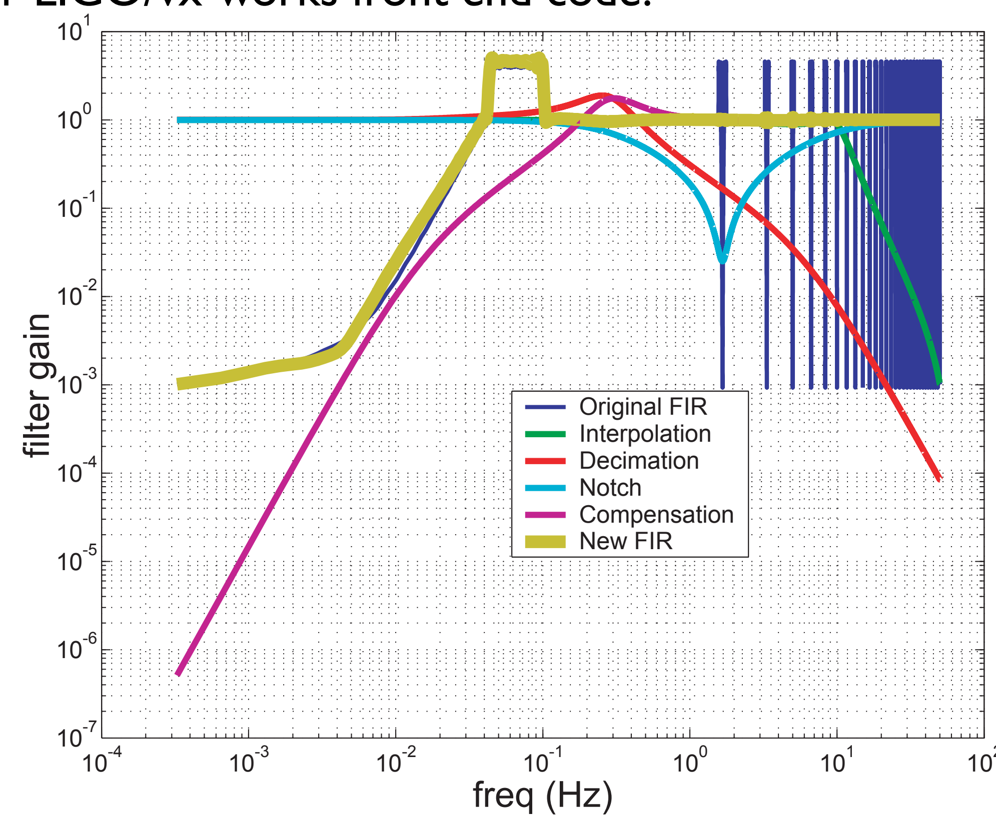

# Vertical and transverse performance

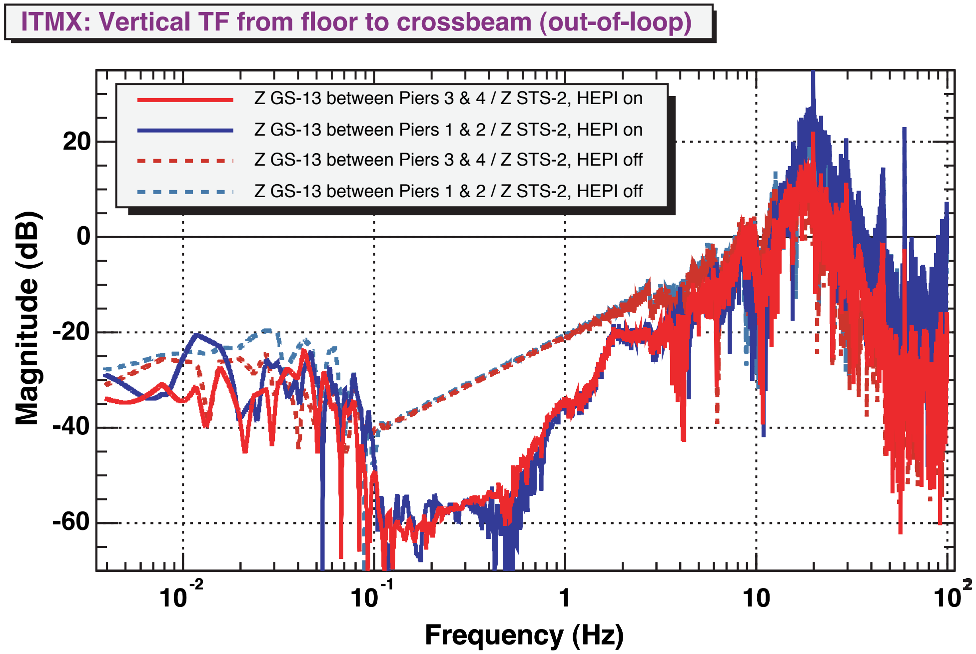


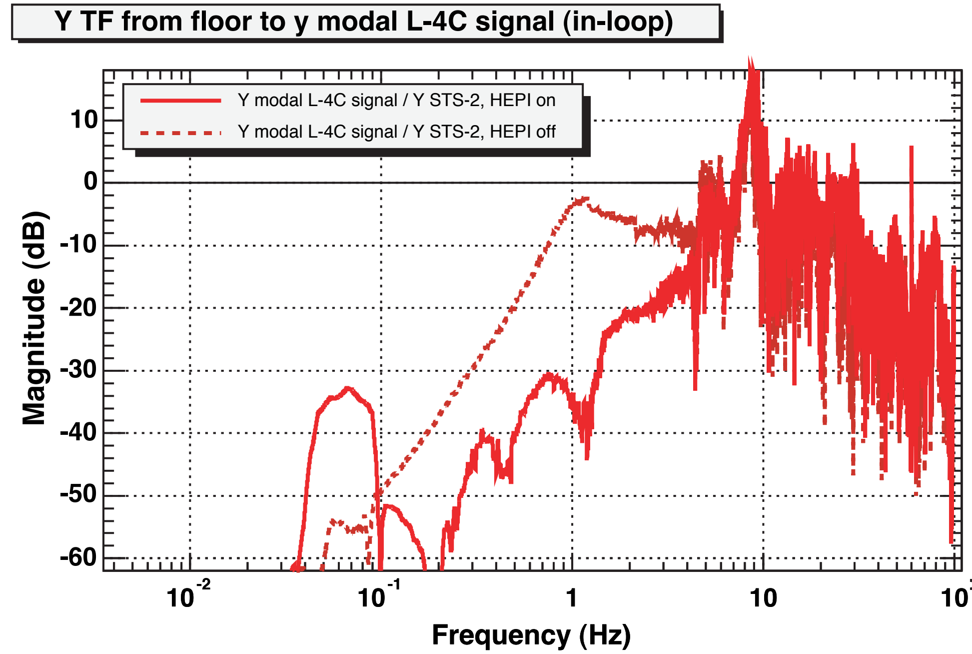


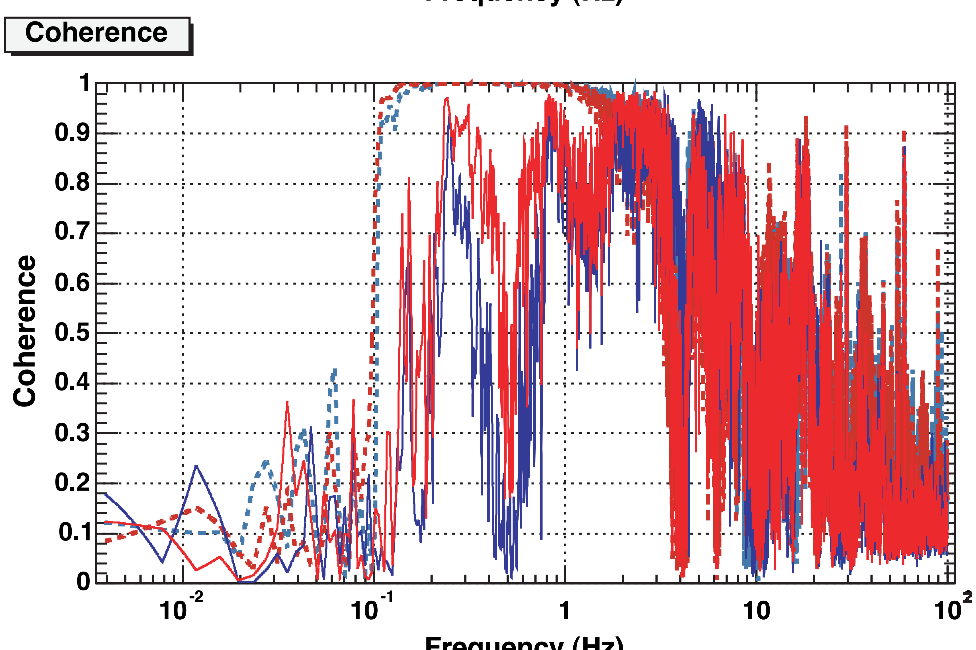


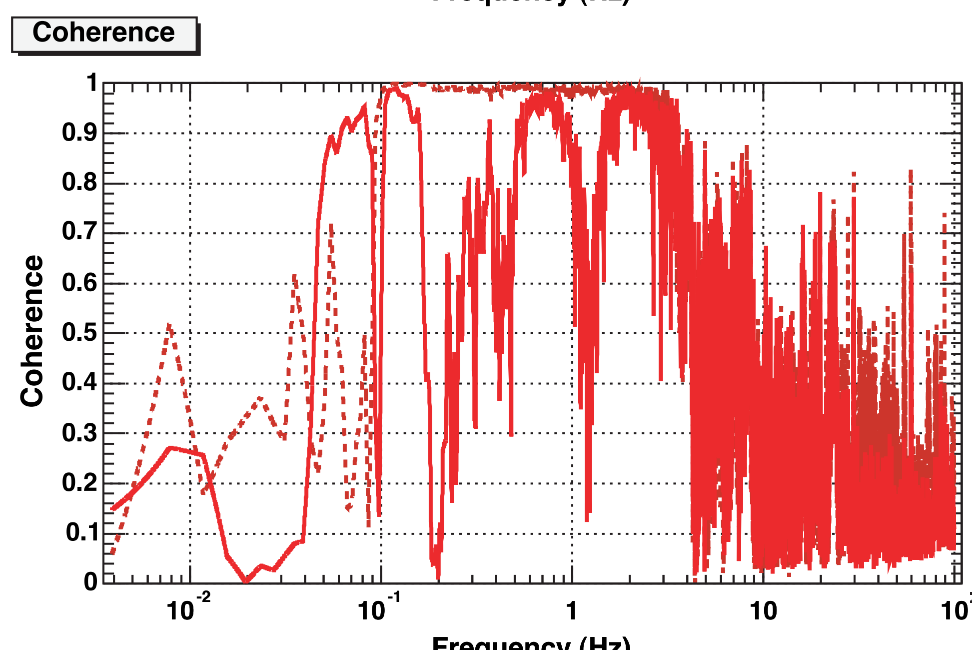

# X, yaw and pos performance

**ITMX: X TF from floor to crossbeam**

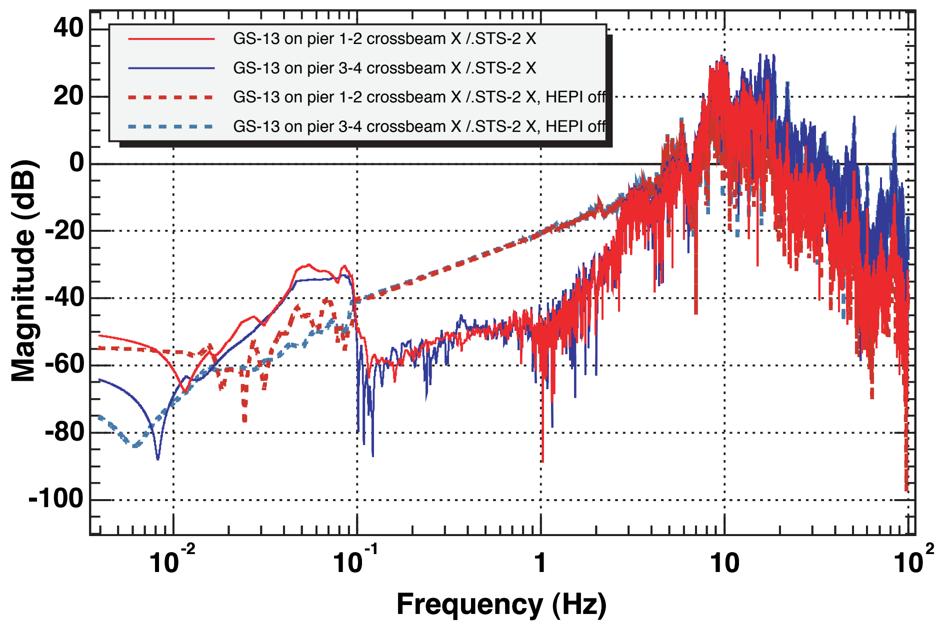


**X noise on crossbeams**

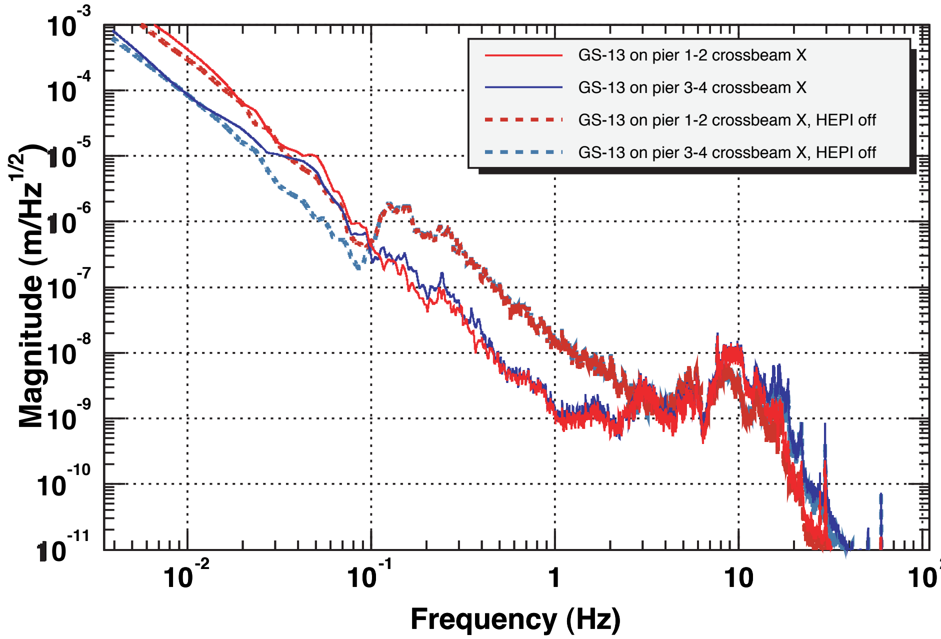


**Yaw optical table noise, from SUSYAW**

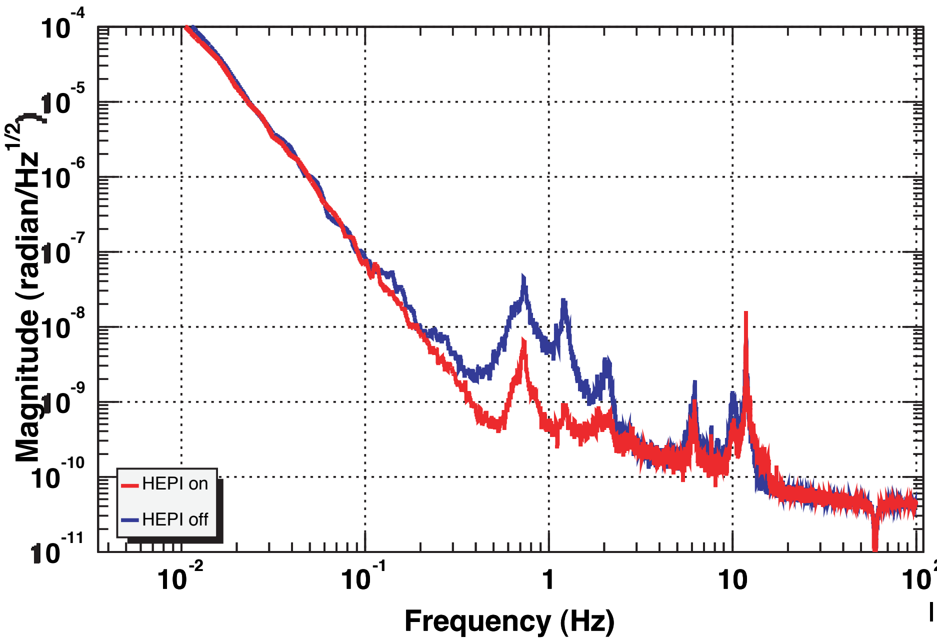


**X optical table noise, from SUSPOS**

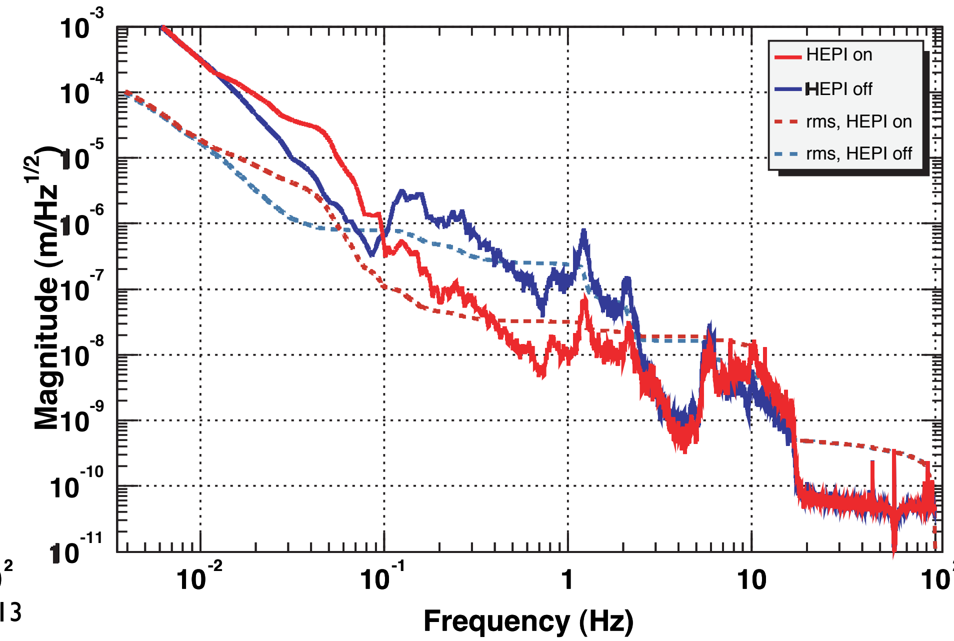

# Detector disturbance levels

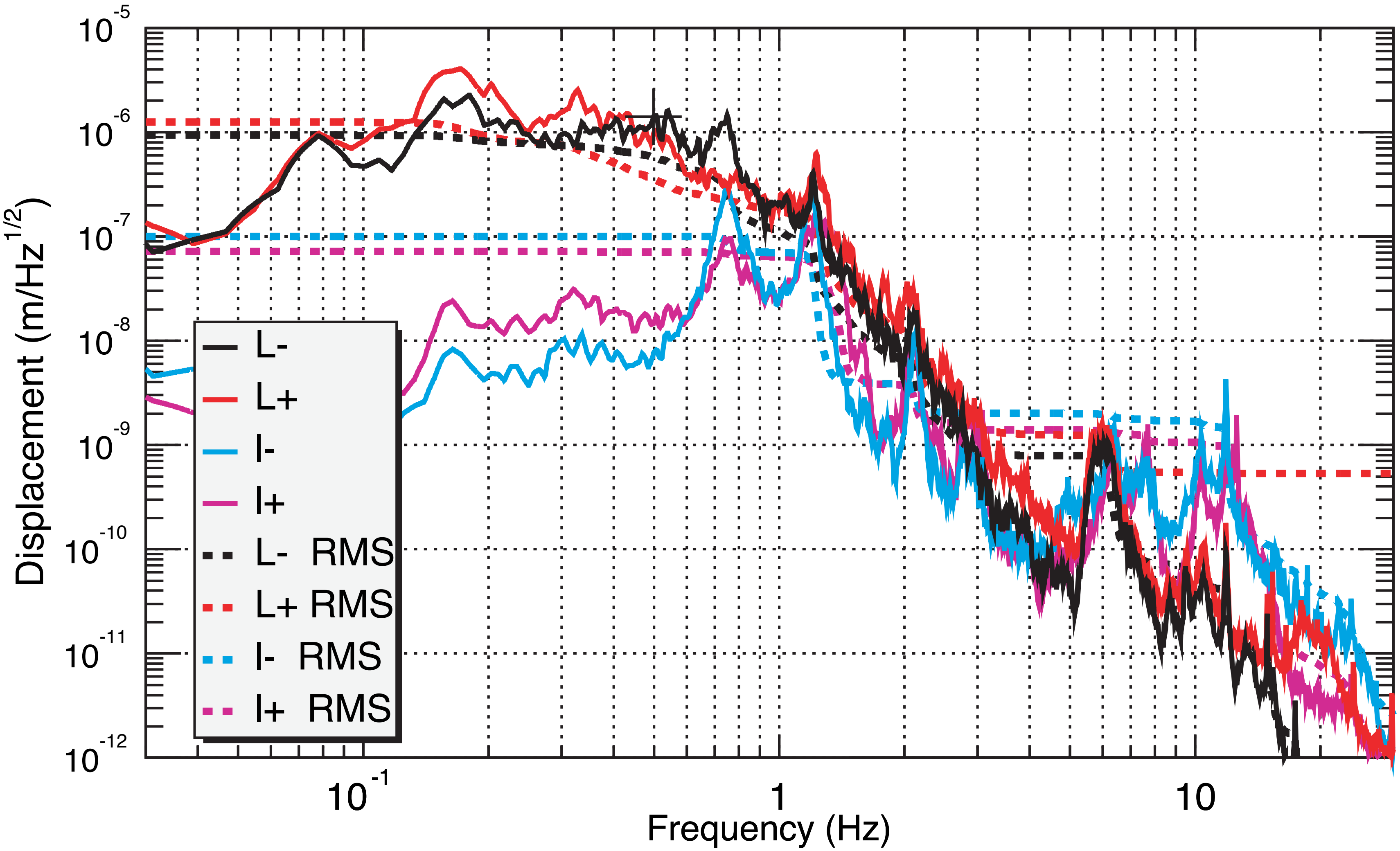


- Data from R. Adhikari's MIT Ph.D. thesis (2004) of the LLO detector.
- Bulk of RMS disturbance comes from 0.1–2.1 Hz band. 1 μm rms is consistent with detector operation. Also, 1 μm/s rms velocity is the practical limit for reliable lock acquisition.

# X-arm length disturbance, quiet evening

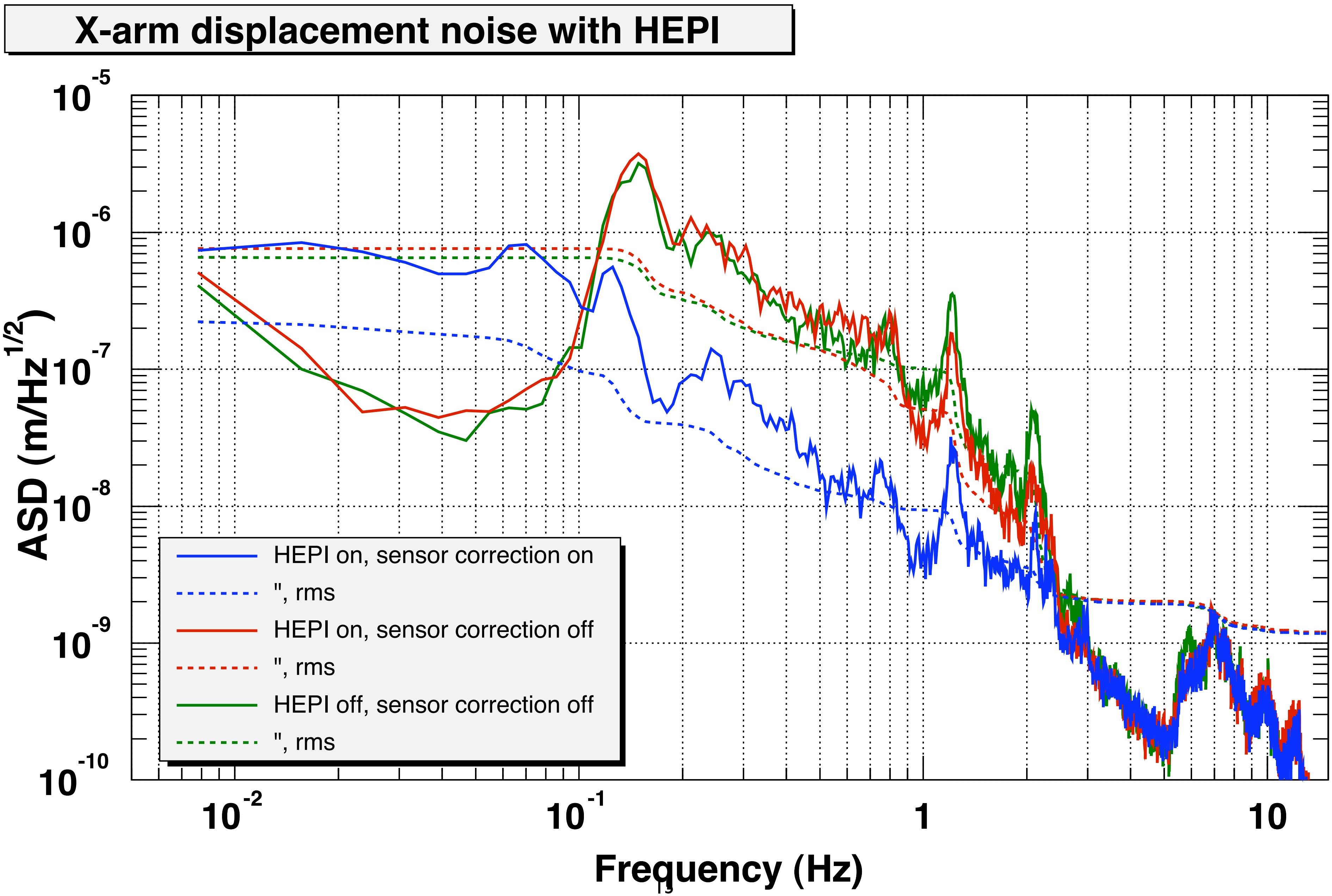

# X-arm length disturbance, quiet evening

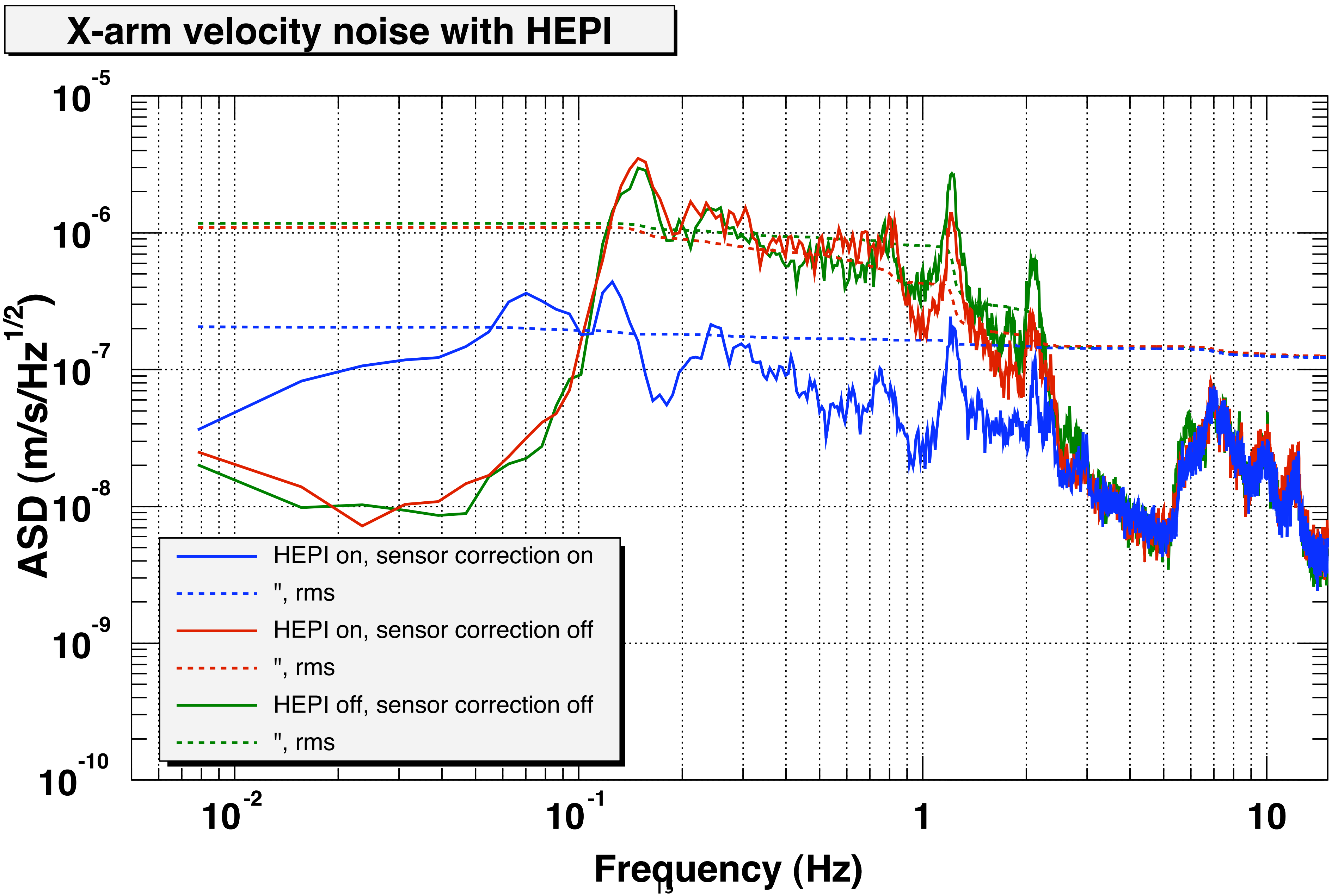

# X-arm length disturbance, noisy afternoon

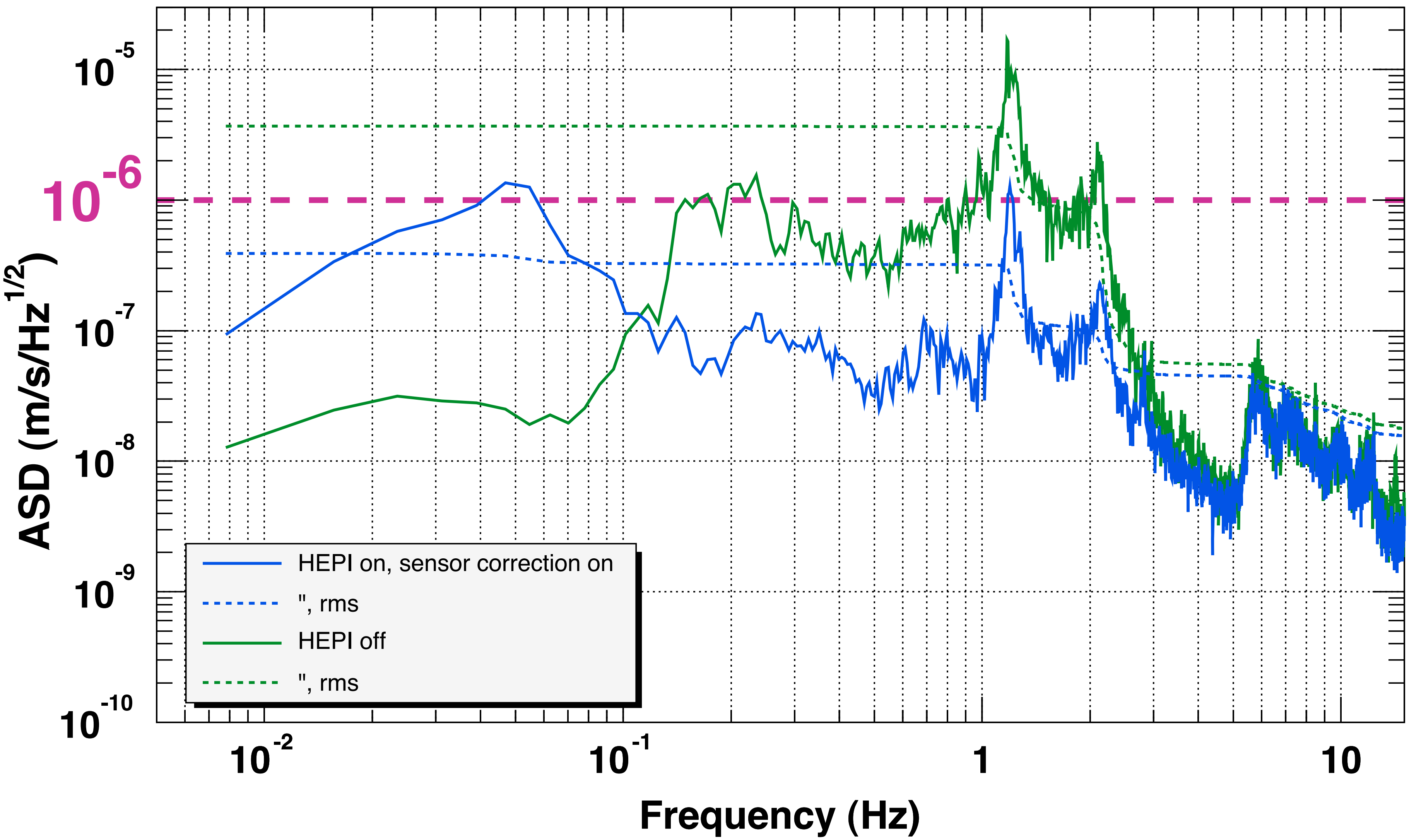


- Noisy afternoon of Aug 10, 2004 had a BLRMS ground velocity 1–3 Hz monitor value between the 90th and 95th percentiles.
- With HEPI in use, we expect the LLO detector to work on such a day, with factor of 2 headroom.

# Band-limited rms velocity monitor statistics

- Analysis of 600+ days of BLRMS data from LIGO PEM seismometers: E. Daw et al, Class. Quantum Grav. **21,** 2255 -2273. (2004)
  - 1–3 Hz: 4–7 *x higher at LLO.*
  - 0.3–1 Hz: *5–7 x higher at LLO.*
  - 0.1–0.3 Hz: *3 x higher at LLO.*

example: 1–3 Hz 90th percentile values

| site | chan | 90%, μm/s | llo/lho |
|---|---|---|---|
| LLO | lvea x | 0.31 | 4.0 |
| | lvea y | 0.29 | 3.6 |
| | ex x | 0.34 | 4.5 |
| | ey y | 0.75 | 7.3 |
| LHO | lvea x | 0.078 | |
| | lvea y | 0.083 | |
| | mx x | 0.077 | |
| | my y | 0.10 | |

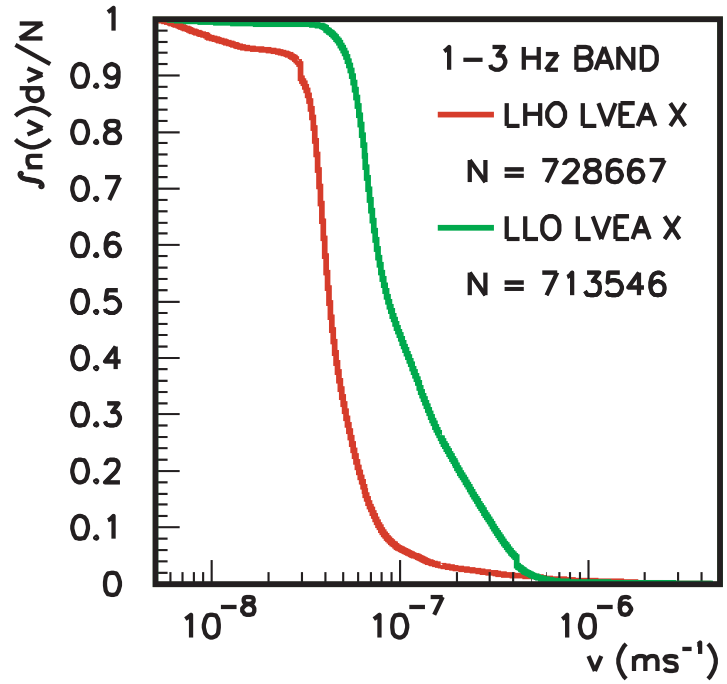


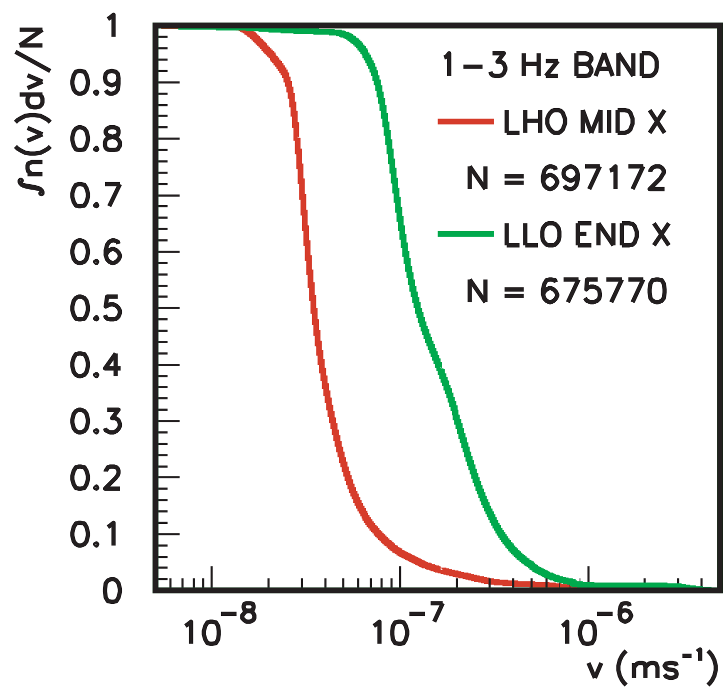

# Torture-test data

- Data taken during very noisy episodes during S2, when we could not reliably lock the LLO detector.
- RMS acceleration, velocity and displacement calculated between 20 mHz and 16 Hz tabulated, for EY Y - EX X + LVEA X - LVEA Y.
- Worst day that we observed, if suppressed by HEPI as currently performing, would probably permit interferometer lock.

| data file | Displacement | Velocity | Acceleration |
|---|---|---|---|
| Enormous µseism | **63 µm p-p** | **35 µm/s p-p** | **180 µm/s$^2$ p-p** |
| | 11 µm rms | **4.8 µm/s rms** | 17 µm/s$^2$ rms |
| Day Train | 13 µm p-p | 13 µm/s p-p | 150 µm/s$^2$ p-p |
| | 1.7 µm rms | 1.6 µm/s rms | 17 µm/s$^2$ rms |
| Borderline day | 30 µm p-p | 18 µm/s p-p | 150 µm/s$^2$ p-p |
| | 4.6 µm rms | 2.5 µm/s rms | 17 µm/s$^2$ rms |

# What about the train?

- Data from day with high microseism, with and without train, looking at EY Y seismometer, which bears the brunt of the train.
- Also, these data show a set of nightmare microseism graphs.
- Train vibration energy falls mainly in the 1–2 Hz band, which is reduced well by HEPI. Some falls just above the HEPI band.

11 AM CST, without train

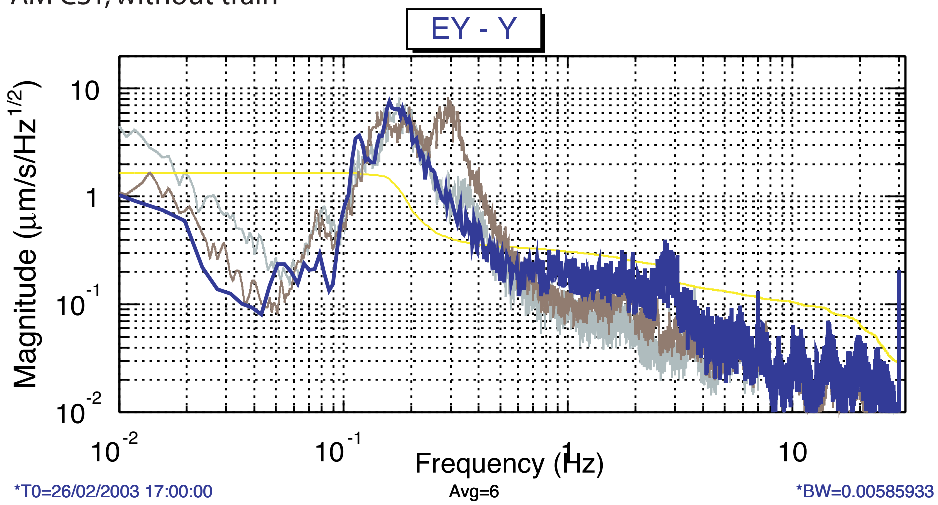


2 PM CST, **with** train

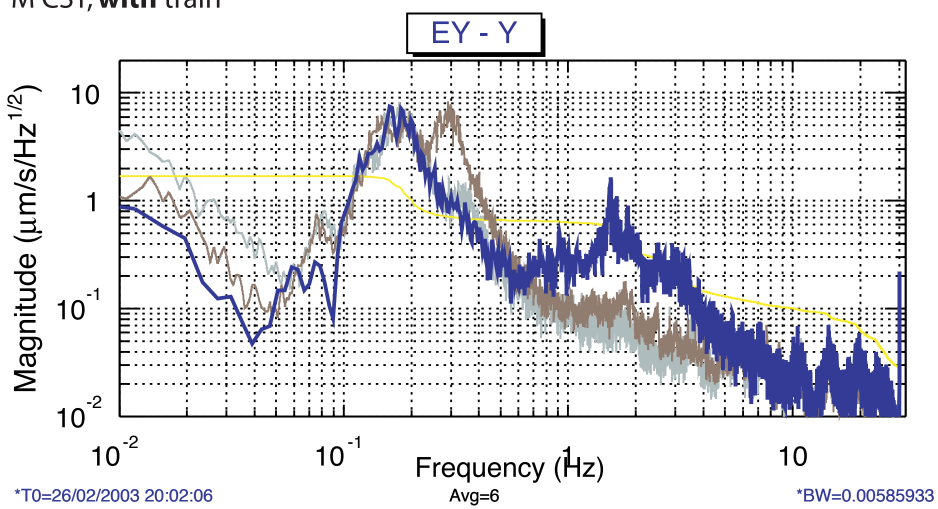

# Remaining tasks

- Complete basic functionality on 6 more payloads
- Optimized sensor gains and whitening to make saturation less likely during extreme storms.
- Lock/unlock scripts, interfaced with watchdog function, to automate HEPI operation.
  - 3-stage watchdog, switches among servo & sensor correction, servo only, offset only, or HEPI off.
  - Simplified operator's EPICS screen.

# Methods for improvement

- Resonant gain in the geophone-based inertial-feedback controller to lower the stack mode excitation, and/or the test mass bounce mode. This is a challenge, as it makes sensor correction filter performance more sensitive to small plant changes, perhaps involving non-minimum phase zeros; we will try it of course.

- Control reallocation from test mass suspension OSEMS to HEPI. This will certainly be done at tidal frequencies, where the blend effects will have only a small effect on sensor correction.

- Adaptive sensor correction, to adjust the correction filter as conditions change. This is under study at LASTI.